Terahertz electromagnetic transitions observed within the $^4I_{15/2}$ ground multiplet of Er^{3+} ions in Si

S. Minissale,[1] N. Q. Vinh,[2] A. F. G. van der Meer,[2] M. S. Bresler,[3,*] and T. Gregorkiewicz[1]
[1]*Van der Waals-Zeeman Institute, University of Amsterdam, Valckenierstraat 65, NL-1018 XE Amsterdam, The Netherlands*
[2]*FOM Institute for Plasma Physics "Rijnhuizen," NL-3430 BE Nieuwegein, The Netherlands*
[3]*A.F. Ioffe Physico-Technical Institute, RAS, 26 Polytekhnicheskaya, 194021 St. Petersburg, Russia*
(Received 23 January 2009; published 31 March 2009)

An optically induced terahertz transition within the crystal-field-split ground state of Er^{3+} ion in Si has been conclusively established. A Si/Si:Er multinanolayer structure, where a single type of Er-related centers dominates, has been used. The study was conducted by pump-probe technique with a free-electron laser. Using the transient grating experimental configuration, we identify an absorption band at $\lambda \approx 43.5$ μm and measure the related effective lifetime as $\tau \approx 50$ ps.

DOI: 10.1103/PhysRevB.79.115324 PACS number(s): 78.55.Ap, 68.55.Ln, 78.47.J−, 78.67.Pt

The 30–300 μm wavelength range, which separates the predominantly optical and predominantly electric domains, is frequently referred to as the "terahertz gap" (1–10 THz). This reflects on the fact that the terahertz range remains poorly explored while almost the entire electromagnetic spectrum is exploited for practical applications, such as optical communications and data storage, spectroscopy, electronics and radiocommunications and telecommunications, radar, and x-ray diagnostics among others. The main reason for this situation is that to date no cheap and practical sources of terahertz radiation have been developed. In fundamental research concerning, e.g., carrier dynamics, the conveniently tunable free-electron lasers (FELs) remain the most popular radiation source. These installations are, however, highly impractical in view of their size and operational costs. Another solution is offered by optically pumped molecular lasers but these are also rather inconvenient with fixed emission wavelengths. At the same time, many interesting applications for terahertz range have been identified; these include remote sensing (molecule identification) and imaging for security and medical diagnostics, and also communications, where the terahertz band offers greater bandwidth and reduced antenna sizes. Therefore research toward development of a compact, versatile, and preferably electrically operated terahertz light source continues.[1]

In that context, a Si-based terahertz laser would be particularly welcome in view of the dominance of Si in contemporary electronics and the unprecedented sophistication of the Si complementary metal-oxide semiconductor (CMOS) technology. Here the possibility to use transitions between shallow donor and acceptor impurity states has been proposed,[2] and stimulated emission from phosphor[3] and arsenic[4] donors in Si has been demonstrated. However these solutions require separate and powerful optical pumping (FEL and CO_2 laser in Refs. 3 and 4, respectively) and cryogenic temperatures. Therefore their projected applications are in space and atmospheric research rather than for the terrestrial concepts mentioned earlier. An alternative solution may be offered by quantum cascade lasers based on III-V compounds, which utilize intraband transitions,[5] but operational temperature range of such devices is strongly hampered by polar-optical phonon scattering. This effect should be absent in Si (and Ge), which are nonpolar materials.[6,7] Consequently concepts of cascade lasers based on (strained) Si-Ge quantum wells have been put forward[8,9] and their realizations are being explored.[10,11]

Rare-earth (RE) ions are frequently used for tailoring optical properties of insulating and semiconducting hosts. For semiconductors, special attention has been given to Er doping of silicon, with the research clearly fuelled by prospect applications in Si photonics and optoelectronics—for a comprehensive review see, e.g., Ref. 12. RE-doped materials have also been considered for generation of terahertz radiation. At a time, it appeared plausible to use for that purpose optical transitions between individual levels within a single spin-orbit multiplet of a RE ion split by a local crystal field. This approach to terahertz generation turned out to be unsuccessful due to large width, and therefore mutual overlap, of emission lines from individual crystal-field-split levels. The situation is considerably different in Si/Si:Er multinanolayer structures grown by sublimation molecular beam epitaxy (MBE),[13] where a single type of Er-related optical centers is preferentially formed.[14–16] The low-temperature photoluminescence (PL) spectrum of this material features a set of very sharp lines with linewidth of $\Delta E < 8$ μeV. In this way, the major obstacle hampering previous attempts of utilizing Si:Er for development of a terahertz source has been removed. In this study, we explore the possibility of optical transitions between the well-defined crystal-field-split sublevels of the $^4I_{15/2}$ ground state of the Er^{3+} ion in a Si/Si:Er multinanolayer structure.

The experiments have been performed on a Si:Er structure comprising 400 alternating Si and Si:Er layers—see Ref. 15 for sample details. As mentioned before, Er^{3+} ions in this sample are preferentially incorporated in a single type of optically active center, designated Er-1, whose emission is characterized by ultranarrow emission lines. The ultrafast (picosecond resolution) pump-probe measurements in the terahertz range have been performed at the Dutch free-electron laser user facility FELIX. All the measurements were done at $T \leq 5$ K with the sample placed in a helium gas flow cryostat. The laser power incident on the sample was $P \approx 50$ mW [as measured at $\lambda_{FEL} = 43$ μm, 1 GHz repetition rate, and 7 μs (macro) pulse duration].

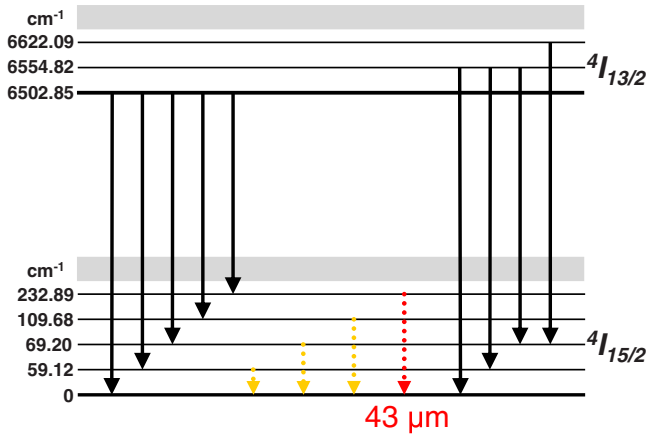

FIG. 1. (Color online) Schematic of the energy-level scheme for the ground and the first-excited states of the Er-1 center. Gray zones indicate energy range where additional thus far unidentified levels should be located. Transitions observed in PL are shown by solid arrows. Dotted arrows indicate possible terahertz transitions within the ground-state multiplet; in red (dark gray), the $\lambda \approx 43$ μm transition investigated in the current study is shown.

In the past, we have precisely determined the crystal-field-induced splitting between sublevels of the ground state of the Er-1 center.[15] This is illustrated in Fig. 1, where also the most prominent PL transitions used to establish this energetic scheme are indicated. On this basis, the wavelengths of the possible terahertz transitions can be predicted. Identification of the $\lambda \approx 43$ μm transition between the levels of the $^4I_{15/2}$ ground state of an Er^{3+} ion—indicated in Fig. 1—is the main subject of this report.

As an initial task, we carried out Fourier transform infrared (FTIR) absorption measurements on our sample in order to demonstrate the presence of a linear absorption band at the $\lambda \approx 43$ μm wavelength of the predicted transition. Unfortunately, no absorption signal has been detected, while the reliability of the experiment was assured by observation of an absorption signal of ≈30% and ≈65%, respectively, for the two boron-related transitions at 40.8 and 35.9 μm. In order to explain the negative result, we note that only ~1–1.5 μm of the total thickness of the sample contains Er, with a concentration of $[\mathrm{Er}]=2\times10^{18}$ cm^{-3}, while B is present with a concentration of $[\mathrm{B}]=2.7\times10^{15}$ cm^{-3} in the ~500-μm-thick substrate on which the Si/Si:Er structure is grown. This implies that the areal density of Er ($N_{\mathrm{Er}} \approx 3\times10^{14}$ cm^{-2}) is of the same order as that of B ($N_{\mathrm{B}} \approx 1.3\times10^{14}$ cm^{-2}). At the same time, however, two further corrections have to be taken into account: (i) the Er transition is forbidden for parity reasons and its probability is 10^2–10^3 times lower when compared to that of B and (ii) not all Er dopants present in the sample will form the Er-1 center and participate in the predicted absorption.[17] Combining these facts, we can expect the absorption by B to be considerably (~2–3 orders of magnitude) stronger than by Er. By inspecting the recorded linear absorption spectrum, we conclude that any Er-related absorption, if present, would be below the background noise level and therefore impossible to detect under conditions of the experiment. Therefore we conclude that the lack of Er-related absorption band in the FTIR spectrum cannot be seen as a decisive argument against the existence of the investigated transition.

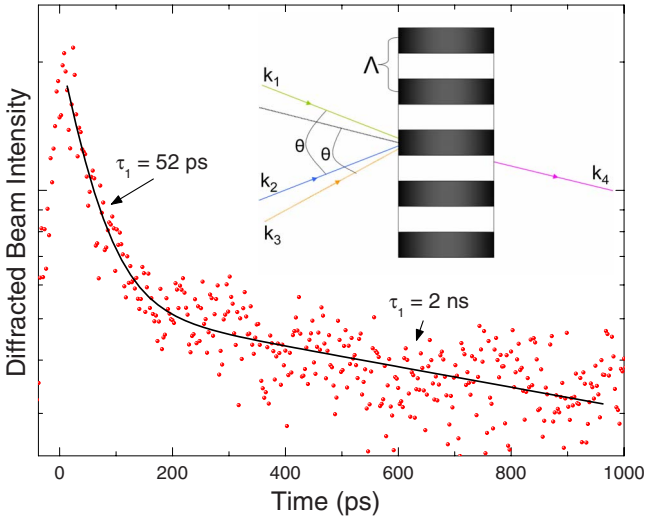

FIG. 2. (Color online) Result of the pump-probe measurement at $\lambda_{\mathrm{FEL}}=43.5$ μm in transient grating configuration. A clear absorption band with a time constant of $\tau_1 \approx 52$ ps can be seen, superimposed on slowly decaying ($\tau_2 \approx 2$ ns) background, possibly of thermal origin. In the inset the interference pattern created on the sample by the split pump beam is shown. The fringe separation Λ depends on the wavelength and the angle between the pump beams θ: $\Lambda = \lambda/2\sin(\theta/2)$.

Consequently, we performed pump-probe experiments in the $\lambda=43$ μm range of the expected transition. In these measurements, an additional parameter appears—the lifetime of the participating excited state. As mentioned before, for Er we are dealing with a forbidden transition, while for B the optical transitions are allowed. However in both cases recombination transition probabilities are likely to be dominated by nonradiative processes, as phonon scattering will prevail over photon emission. On the other hand, we can expect a considerable difference of the Huang-Rhys factor for B and Er, resulting in different coupling to lattice phonons. The experiment has been performed in the *transient grating* configuration. In this case, the FEL beam is split into three parts by two polymer beam splitters (PP and Mylar): two "pump" beams (having wave vectors $\mathbf{k}_1$ and $\mathbf{k}_2$) and a "probe" beam, having wave vector $\mathbf{k}_3$—see inset of Fig. 2. The two pump beams are spatially and temporally overlapped on the sample. Using a small angle of incidence for the two pump beams and moving the sample up and down, the grating can be "inserted" into the structure. In that way the part of the sample closer to the surface can be selected, thus reducing the substrate contribution and giving advantage to the Er-doped top layer. Consequently, the Er-related contribution relative to that of boron could be more pronounced than in case of direct absorption. If the FEL is resonant with an absorption transition available in the sample, then the resulting excitation is spatially modulated across the overlap region, resulting in a population grating. The weaker beam $\mathbf{k}_3$, spatially overlapped but time delayed, is then Bragg diffracted off this grating into a phase-matched signal direction ($\mathbf{k}_s=\mathbf{k}_1-\mathbf{k}_2+\mathbf{k}_3$). By scanning the time delay

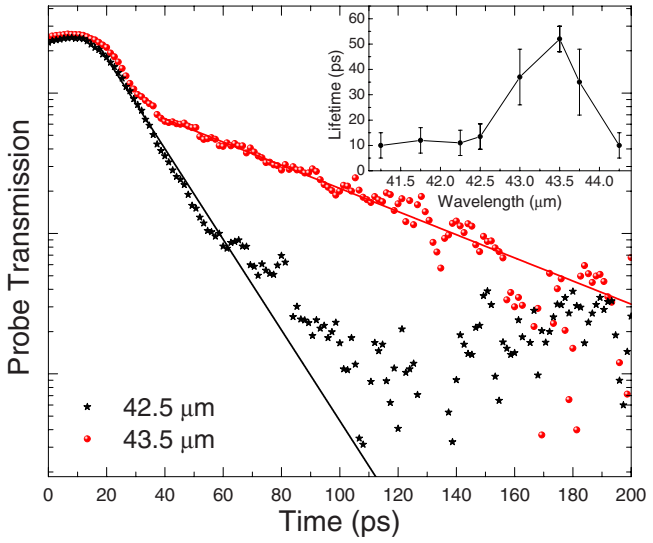

FIG. 3. (Color online) Comparison of the transmission signal experimentally measured off and on resonance at 42.5 (black stars) and 43.5 μm (red spheres), respectively. Solid lines correspond to decay time constants of 10 and 50 ps. In the inset, wavelength dependence of the time constant dominating the decay of absorption detected in the pump-probe experiment is shown (standard three-beam configuration).

Δt of the probe pulse with respect to the pump pulses, the amplitude of the population grating can be measured as a function of time. The grating decays as $\exp(-2t/\tau)$, where τ corresponds to the time constant characteristic of the absorption transition generating the grating. In that way, the lifetime of the excited state can be measured. The transient grating technique has the important advantage of being practically background free; the diffracted signal appears only when the grating is formed due to absorption in the structure.[18] In that way the appearance of any additional signals, not directly related to the investigated absorption, is avoided.

The pump-probe experiments performed in the transient grating configuration at the FEL wavelength of $\lambda=43.5$ μm revealed a clear absorption feature, as depicted in Fig. 2. From this measurement, the relevant decay time constant of $\tau=50\pm5$ ps was concluded. The slower, $\tau_2\approx2$ ns component observed simultaneously, represents most probably the heating effect, commonly seen in that configuration.[19] Measurements performed at other wavelengths in that range (at 0.5 μm steps, not shown) yielded no absorption signal, thus evidencing the resonant character of the detected band.

The resonant aspect of the identified absorption band was further investigated in detail in a standard pump-probe reference configuration (see, e.g., Ref. 20 for experimental details). The results are shown in Fig. 3. In the main panel, the (normalized) traces for two wavelengths of $\lambda=43.5$ and 42.5 μm, i.e., "on" and "off" resonance, are compared. For $\lambda=43.5$ μm, the previously identified absorption band with τ (50 ± 5 ps) can again be seen. In that case, however, it appears superimposed on a faster decaying signal, characterized by a time constant of $\tau_F\approx10$ ps. In the inset of Fig. 3, we show the wavelength dependence of the time constant dominating the absorption. As can be seen, the slow 52 ps component is indeed resonant, centered around $\lambda\approx43.5$ μm. A similar measurement performed on a B-doped Er-free sample did not reveal any resonances in that wavelength range. Consequently, we identify it with the expected ground-state transition of Er^{3+}. The origin of this fast component, which appeared in the whole investigated wavelength range and which was absent in the transient grating configuration, is not clear at this point and will not be considered further. For comparison, as for the FTIR absorption, we performed a similar experiment for the B-related band at $\lambda=40.8$ μm. A clear absorption with the characteristic decay time of $\tau\approx70$ ps (Ref. 21) has been observed. The amplitude of the B-related signal was approximately 50 times larger than that measured at $\lambda=43.5$ μm. This implies that the 43.5 μm band represents absorption of approximately 0.5%, too small to be disclosed in the FTIR measurement.

From the above presented experimental evidence we conclude that an optical transition within the $^4I_{15/2}$ ground state of the Er^{3+} ion involved in the Er-1 center has been observed. We will now address the origin of the determined time constant. The theory of interaction of RE ions with lattice vibrations has been considered in the past. The lifetime of the upper (doublet) level is determined by spontaneous phonon emission,

$$\tau_p^{-1}=\frac{1}{\pi\hbar\rho v^2}\Phi_{mm'}\frac{\omega^3}{v^3}, \tag{1}$$

where ω is the frequency of the emitted phonon, given by the energy difference ΔE between the two states involved in the transition $\hbar\omega=\Delta E$. The matrix element of the RE ion-phonon interaction is determined by the matrix elements of Stevens operators,

$$\Phi_{mm'}=3\sum_{n,M}(\chi_n A_n^M)^2|\langle Jm|\hat{O}_n^M|Jm'\rangle|^2. \tag{2}$$

The constants $A_n^M=g_n^M A_n^0$ play the same role as deformation potentials in the theory of semiconductors—see Ref. 22 for the notation. Using also the values of the relevant quantities given in this reference, we can estimate the lifetime of the Er^{3+} ion in the upper state of the ground multiplet as $\tau_p\approx12\times10^{-12}$ s (where we have used the sound velocity averaged over three acoustic branches $v\approx6\times10^5$ cm/s). We have included only the transitions from the upper-doublet-to-the-lowest-doublet state, since, as can be concluded from Eq. (1), the probabilities of the transitions to the closer doublets diminish as a cube of energy difference. We see that in spite of the very crude treatise, our result is of the same order as the experimental value of 50 ps.

The radiative lifetime for the transition from the upper to the lower doublet level is given by

$$\tau_{sp}^{-1}=\frac{e^2\bar{n}d_{12}^2\omega^3}{3\pi\epsilon_0\hbar c^3}, \tag{3}$$

where now ω is the frequency of the emitted photon (again given by the energy difference ΔE), $\bar{n}$ is the refractive index, c is the light velocity, ϵ_0 is the dielectric constant of vacuum,

and d_{12} is the dipole matrix element. We remark that the factor ω^3 in Eq. (3) appears since the emission rate is proportional to the photon density of states ($\sim\omega^2$) but also to the square of the electric field of emitted light, i.e., to the photon stream ($\sim\omega$)—see, e.g., Ref. 23. Since the nonzero probability values for the $f-f'$ radiation transitions are obtained only due to the admixture of d states to the f states of an Er^{3+} ion, we can expect that the matrix elements are of the same order of magnitude for ${}^4I_{13/2}\rightarrow{}^4I_{15/2}$ transition and within the ${}^4I_{15/2}$ multiplet. Therefore, the difference in the radiation lifetimes for these transitions should be determined mainly by the photon density of states, i.e., by the cube of the ratio of the corresponding energies (equal to ~ 30). Consequently, assuming ~ 10 ms lifetime for the ${}^4I_{13/2}$ excited state of Er^{3+}, the radiative lifetime of the upper-doublet-to-lower-doublet transition can be estimated as $\tau_s \approx 10^{-2}\times 2.7\times 10^4 = 270$ s. These estimates rule out the possibility of the experimentally measured lifetime being the radiative one; consequently, we identify it as being due to the nonradiative multiphonon recombination.

It is interesting to compare the current findings with the previously mentioned work on impurity level recombination of shallow dopants in silicon. In that case the relation between nonradiative and radiative recombination time constants is important. For Si:P, where realization of stimulated emission has been reported,[3] the nonradiative recombination lifetime of $\sim$200 ps has recently been measured.[24] This value is in good agreement with the present finding. As for the radiative recombination, the exact value for P is not known, and values of up to 10^{-3} s have been reported.[25] These values are considerably shorter than our estimate for Er, since the $1s\rightarrow 2p$ optical transition of P is allowed. On the other hand, the f character of electronic functions involved in the Er transition could bring the advantage of a smaller linewidth; to this end we note that the width of the $2p_0$ absorption band for Si:P (in an isotopically pure ${}^{28}Si$ sample) has been established as $\Delta E = 4.2$ μeV,[26] while for the Er transition only the upper limit of $\Delta E < 8$ μeV is known at present, and a much smaller value of the linewidth can be expected.

In summary, the presented results conclusively identify an optically induced transition within the ${}^4I_{15/2}$ ground state of an Er^{3+} ion in Si/Si:Er multinanolayer structure. The transition is observed in absorption at $\lambda \approx 43.5$ μm. At a liquid-helium temperature, the relevant relaxation lifetime is determined as $\tau \approx 50$ ps. We argue that this value reflects a nonradiative multiphonon recombination process. While past investigations of Si:Er have concerned the 1.5 μm band relevant for telecommunications, the current result demonstrates that the nanoengineered Si:Er could also be relevant for the terahertz range. One attractive possibility could be to develop and explore plasmonic waveguides based on Si/Si:Er multinanolayers and in that way enhance the radiative recombination of Er^{3+} ions,[27] but for practical applications also ways to decrease nonradiative recombinations should be designed.

This work is part of the research program of the Stichting voor Fundamenteel Onderzoek der Materie-FOM financially supported by NWO. We also gratefully acknowledge the financial support of the European Research Office, support of FOM in providing FELIX beamtimes, and skillful assistance from FELIX staff. The SMBE-grown multinanolayer structure used in this study was kindly provided by Z. Krasil'nik from the Institute for Physics of Microstructures, RAS under Dutch-Russian collaboration program sponsored by NWO.

*Deceased.

[1] A. Borak, Science **308**, 638 (2005).

[2] E. E. Orlova, R. Ch. Zhukavin, S. G. Pavlov, and V. N. Shastin, Phys. Status Solidi B **210**, 859 (1998).

[3] S. G. Pavlov, H. W. Hubers, J. N. Hovenier, T. O. Klaassen, D. A. Carder, P. J. Phillips, B. Redlich, H. Riemann, R. K. Zhukavin, and V. N. Shastin, Phys. Rev. Lett. **96**, 037404 (2006).

[4] H.-W. Hübers *et al.*, Appl. Phys. Lett. **84**, 3600 (2004).

[5] R. Köhler *et al.*, Nature (London) **417**, 156 (2002).

[6] P. Murzyn *et al.*, Appl. Phys. Lett. **80**, 1456 (2002).

[7] M. Califano *et al.*, Phys. Rev. B **75**, 045338 (2007).

[8] L. Friedman, R. A. Soref, and G. Sun, J. Appl. Phys. **83**, 3480 (1998).

[9] R. A. Soref and G. Sun, Appl. Phys. Lett. **79**, 3639 (2001).

[10] S. A. Lynch *et al.*, Appl. Phys. Lett. **81**, 1543 (2002).

[11] A. De Rossi, M. Carras, and D. J. Paul, IEEE J. Quantum Electron. **42**, 1233 (2006).

[12] A. J. Kenyon, Semicond. Sci. Technol. **20**, R65 (2005).

[13] V. P. Kuznetsov *et al.*, Phys. Status Solidi A **127**, 371 (1991).

[14] N. Q. Vinh, H. Przybylińska, Z. F. Krasil'nik, and T. Gregorkiewicz, Phys. Rev. Lett. **90**, 066401 (2003).

[15] N. Q. Vinh, H. Przybylińska, Z. F. Krasil'nik, and T. Gregorkiewicz, Phys. Rev. B **70**, 115332 (2004).

[16] I. Izeddin, M. A. J. Klik, N. Q. Vinh, M. S. Bresler, and T. Gregorkiewicz, Phys. Rev. Lett. **99**, 077401 (2007).

[17] We point out that the number of Er dopants participating in the absorption band investigated here is likely to be (substantially) higher than the so-called "optically active" (Ref. 28) part [2–25% for the investigated structure (Ref. 29)].

[18] The transient grating will also appear due to the change in the refractive index, as a follow up of nonresonant effects involving virtual transitions. These, however, will exist only when the electromagnetic field is present, and therefore will reflect temporal characteristics of the laser pulse responsible for the generation of the transient grating.

[19] C. Högemann, M. Pauchard, and E. Vauthey, Rev. Sci. Instrum. **67**, 3449 (1996).

[20] K. K. Kohli, G. Davies, N. Q. Vinh, D. West, S. K. Estreicher, T. Gregorkiewicz, I. Izeddin, and K. M. Itoh, Phys. Rev. Lett. **96**, 225503 (2006).

[21] N. Q. Vinh (unpublished).

[22] R. C. Mikkelson and H. J. Stapleton, Phys. Rev. **140**, A1968 (1965).

[23] M. Fox, *Optical Properties of Solids* (Oxford University Press, Oxford, 2001), p. 269.
[24] N. Q. Vinh *et al.*, Proc. Natl. Acad. Sci. U.S.A. **105**, 10649 (2008).
[25] E. E. Orlova *et al.*, Physica B **302-303**, 342 (2001).
[26] D. Karaiskaj, J. A. H. Stotz, T. Meyer, M. L. W. Thewalt, and M. Cardona, Phys. Rev. Lett. **90**, 186402 (2003).
[27] J. Bao *et al.*, Appl. Phys. Lett. **91**, 131103 (2007).
[28] O. B. Gusev, M. S. Bresler, P. E. Pak, I. N. Yassievich, M. Forcales, N. Q. Vinh, and T. Gregorkiewicz, Phys. Rev. B **64**, 075302 (2001).
[29] N. Q. Vinh, S. Minissale, H. Vrielinck, and T. Gregorkiewicz, Phys. Rev. B **76**, 085339 (2007).